Molecular imaging of plaque inflammation: Tahara and colleagues provide an overview of ^{18}F-FDG and ^{99m}Tc-annexin-A5 imaging in the setting of acute cardiac events and look at the advantages and clinical feasibility of molecular imaging in atherosclerosis. . . . . ***Page 331***

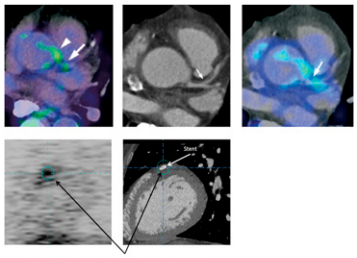

PET in diabetes assessment and monitoring: Fagan and Fischman offer a perspective on recent PET advances in quantifying pancreatic β-cell mass and function and preview an article on this topic in this issue of *JNM*. . . . . ***Page 335***

Methodologies for technology evaluation: Chisin describes the utility and limitations of cost effectiveness and decision analysis approaches in health care as background for an article on ^{99m}Tc-sestamibi imaging in lung cancer in this issue of *JNM*. . . . . ***Page 338***

PET/CT in osteosarcoma prognosis: Costelloe and colleagues look at changes in maximized standardized uptake value and total lesion glycolysis on ^{18}F-FDG PET/CT before and after initial chemotherapy for osteosarcoma as potential indicators of outcomes. . . . . ***Page 340***

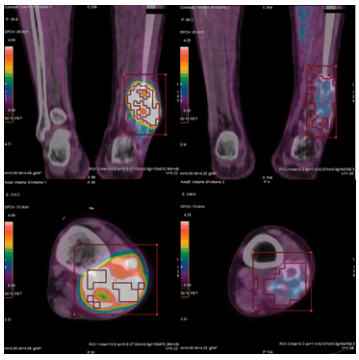

Optimizing PiB PET brain imaging: McNamee and colleagues examine regional Pittsburgh compound B standardized uptake value ratios across 9 injection-to-imaging time windows to establish optimal trade-offs between bias, correlation, and effective contrast in amyloid-β evaluation. . . . . ***Page 348***

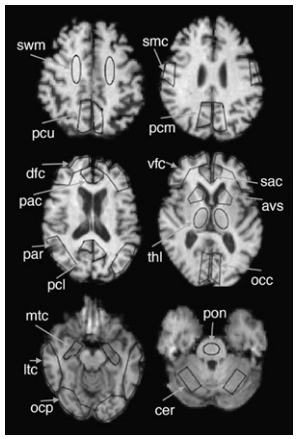

Tryptophan metabolism in lung tumors: Juhász and colleagues explore the in vivo kinetics of the PET tracer α-^{11}C-methyl-L-tryptophan in human lung tumors and discuss the potential of this approach for personalized treatment strategies. . . . . ***Page 356***

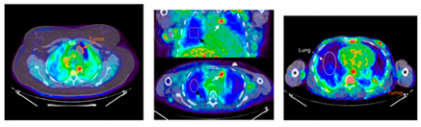

SPECT/CT of lymphatic rerouting: Leijte and colleagues visualize tumor blockage and rerouting of lymphatic drainage in patients with penile cancer and palpable groin metastases and highlight the potential for more accurate sentinel node procedures. . . . . ***Page 364***

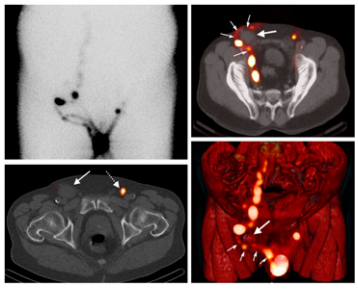

CAD in bone scans: Sadik and colleagues investigate whether a computer-assisted diagnosis system can improve performance and reduce interobserver variation in bone scan determinations of the presence of bone metastases from breast or prostate cancer. . . . . ***Page 368***

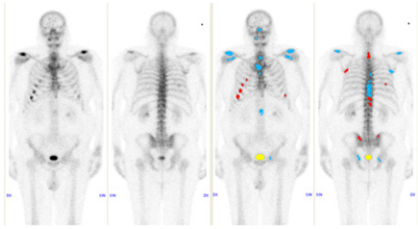

^{99m}Tc-MIBI cost-effectiveness in lung cancer: Mohan and Miles report on a study of the cost-effectiveness of ^{99m}Tc-MIBI SPECT imaging in assessing treatment resistance and predicting response to chemotherapy in patients with lung cancer. . . . . ***Page 376***

PET pancreatic imaging in diabetes: Goland and colleagues assess the feasibility of ^{11}C-DTBZ PET quantification of pancreatic vesicular monoamine transporter type 2 binding in healthy subjects and patients with long-standing type 1 diabetes. . . . ***Page 382***

Perfusion in dilated cardiomyopathy: Range and colleagues analyze myocardial perfusion PET results from patients with nonischemic dilated cardiomyopathy with and without idiopathic atrial fibrillation. . . . . ***Page 390***

HYNIC-TOC in extraadrenal pheochromocytoma: Chen and colleagues compare the imaging efficacy of this ^{99m}Tc-labeled octreotide with that of ^{131}I-MIBG in the evaluation of suspected extraadrenal pheochromocytoma. . . . . ***Page 397***

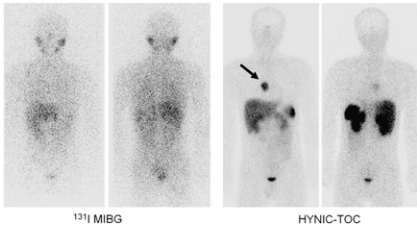

Evaluation of Inveon DPET: Bao and colleagues report on the standards-based performance of this dedicated preclinical PET scanner for high-resolution and high-sensitivity murine model imaging. . . . . ***Page 401***

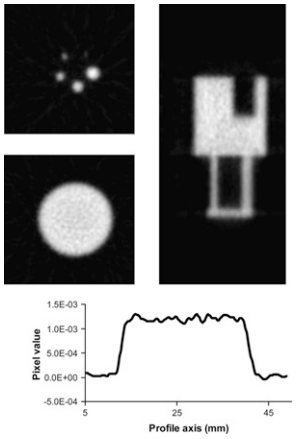

PET imaging with HSV1-tk(A168H) variant: Najjar and colleagues investigate the potential of wild-type herpes simplex virus-1 thymidine kinase and a related mutant as PET reporter genes for dual-tracer imaging of molecular–genetic events in a single subject. . . . . ***Page 409***

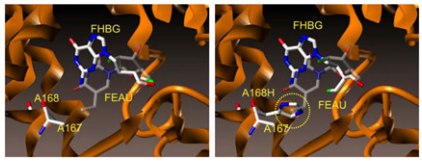

HER2 PET and Affibody molecules: Orlova and colleagues develop and compare 2 epidermal growth factor receptor type 2 PET tracers in vitro and in mice: a ^{124}I-labeled monoclonal antibody and the radiolabeled Affibody molecule, a small-scaffold protein. . . . . ***Page 417***

HBP-1 peptide for head and neck tumors: Nothelfer and colleagues characterize a peptide affine for squamous cell carcinomas of the head and neck with the potential for enhancing diagnostic procedures and tumor-targeted therapies. . . . . ***Page 426***

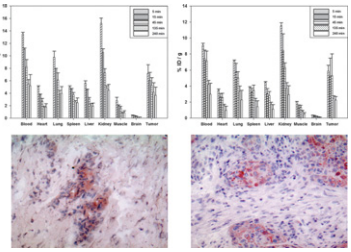

Antimindin antibody fragments: Schneider and colleagues detail in a prostate tumor model the biodistribution and tumor localization of four ^{111}In- and ^{86}Y-labeled antibody formats derived from a single antimindin/RG-1 monoclonal antibody. . . . . ***Page 435***

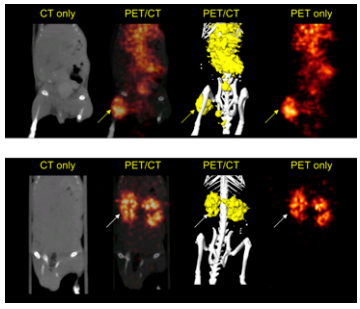

Combined consolidation therapy for NHL: Sharkey and colleagues investigate experimental lymphoma responses using either a bispecific antibody that pretargets ^{90}Y-hapten-peptide radioimmunotherapy or a directly radiolabeled, humanized, ^{90}Y-anti-CD20 IgG in combination with various unlabeled humanized antibodies. . . . . ***Page 444***

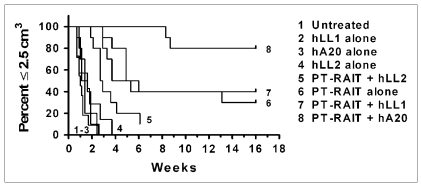

^{99m}Tc(CO)$_3$-nitrilotriacetic acid renal tracer: Lipowska and colleagues describe the development and initial validation of a tracer designed to measure effective renal plasma flow as accurately as ^{131}I-orthoiodohippurate but with better visualization and lower radiation dose to the kidneys. . . . . ***Page 454***

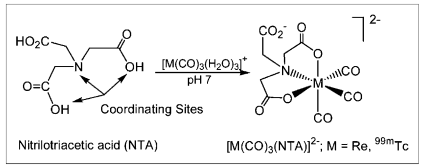

Automatic input function in brain PET: Zanotti-Fregonara and colleagues compare 3 algorithms of automated internal carotid segmentation in human brain PET images with potential application for estimation of image-derived input function. . . . . ***Page 461***

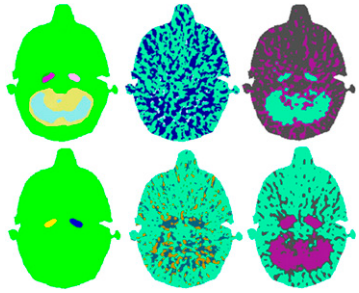

Brain inflammation imaging with PET: Chauveau and colleagues report on 2 new radioligands, both belonging to the pyrazolopyrimidine class, in in vitro and in vivo studies in a rodent model of neuroinflammation. . . . . ***Page 468***

MIRD Pamphlet No. 21: Bolch and colleagues review the latest MIRD schema for assessment of absorbed dose, discuss the need for standardization of nomenclature, and address specific steps required to enhance dosimetry standards for targeted radionuclide therapy. . . . . ***Page 477***

Proposed unit for deterministic effects: Sgouros and members of the MIRD Committee cite the need for a well-defined dosimetry formalism in therapeutic applications of radionuclides and propose a new named unit, the barendsen (Bd), for expression of isoeffective dose. . . . . ***Page 485***

ON THE COVER

^{11}C-dihydrotetrabenazine PET may allow measurement of vesicular monoamine transporter type 2 binding in the pancreas, and preclinical experiments suggest that such measurements may serve as a biomarker of β-cell mass. These images of a patient with type 1 diabetes (top) and a healthy person (bottom) define and separate the pancreas from other abdominal organs.

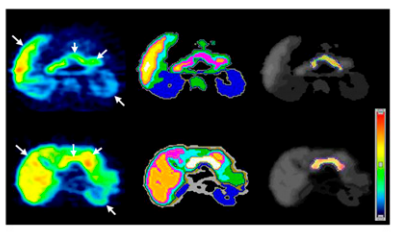

See page 386.